JOURNAL OF MATERIALS SCIENCE **34** (1999) 2121–2133

Mechanical characterisation of glass fibres as an indirect analysis of the effect of surface treatment

P. ZINCK[‡], M. F. PAYS[§], R. REZAKHANLOU[§], J. F. GERARD[‡*]
[‡]*Laboratoire des Matériaux Macromoléculaires, UMR 5627 CNRS, Institut National des Sciences Appliquées de Lyon—Bât 403, 69621 Villeurbanne Cedex, France*
[§]*EMA, DER, Centre de Recherche EDF des Renardières, 77250 Moret-sur-Loing, France*

Tensile strength of E-glass fibres have been analysed using a bimodal Weibull two parameter cumulative distribution function. The bimodal character were associated to surface and internal flaws, respectively. Influence of silane coating as well as industrial sizing on the flaws distribution was quantitatively characterised. A qualitative interpretation of their effect based on a combination of probabilistic and deterministic approaches were proposed in terms of crack healing. It was demonstrated there that mechanical testing of fibres can be used as an indirect observation technique of the consequences of the surface treatment. An analogy is proposed between the sizing treatment of glass fibres and the strengthening of silica glass by means of hybrid organic-inorganic coatings.

1. Introduction

Glass fibre based composite materials became very attractive materials in many areas of industrial applications because of their excellent mechanical performances/cost ratio. Many studies have been performed in recent years on the role of the interface/interphase region in determining the mechanical properties of these materials. The structure of this region depends mostly on the coating applied on the fibre surface before association with a polymer matrix [1].

The sizing has to protect the fibre during handling, and to improve the wettability of the fiber surface by the liquid resin. It generally consists of a water-based mixture containing a lubricant, a film former, and a coupling agent. In most cases, the latter one is an organofunctional alkoxysilane which can react at the glass surface with the silanol groups and favour the chemical coupling with the sizing as well as with the polymer matrix in order to promote the interfacial adhesion. The sizing formulation is applied from an aqueous emulsion (e.g. epoxy, poly(vinyl acetate), etc.) or a solution [1].

It is generally assumed that the interaction between organosilane coupling agents and glass fibres results in a three-dimensional graded network on the glass surface [2, 3]. A study on a deposit of γ-aminopropyltriethoxysilane (or γ-APS) using ToF-SIMS and XPS by Wang and Jones [2] confirmed a structure based on three layers from the glass surface:

- a hydrolytically resistant grafted "interfacial" layer which remains grafted after a hot water or toluene extraction
- a chemisorbed tridimensional layer of polysiloxane
- a physisorbed layer of γ-APS oligomers

The physical and mechanical properties of this network depends on the nature of the silane deposited from the aqueous solution; i.e. amount of coupling agent, pH, rate of hydrolysis and condensation, drying and the conditions used for the sizing treatment [4].

The structure of the sizing layer obtained from the industrial processing is not wellknown, although it is assumed that the silane migrates to the interface providing an interfacial region which is similar to that obtained from the pure coupling agents solutions [1].

The effect of the coupling agent and the other components of the sizing, and as a consequence the structure of the interfacial zones on the interfacial shear stress of the glass fibre/matrix interface has been reported in numerous papers. The interface was studied by the means of micromechanical tests (fragmentation test [5–7], pull-out [8, 9] microbond [10], indentation [11]) as well as macroscopic mechanical testings such as torsion [12], off-axis tension test [13, 14], or *in-situ* studies [15] performed on unidirectional composite materials. The fragmentation test which is widely used in the literature requires the knowledge of the tensile strength at the critical length of the fibre fragments. Since

*Author to whom all correspondence should be addressed.

mechanical testing at such small length (typically from 0.1 to few milimeters) is very difficult, the tests are performed at higher gauge lengths and extrapolation techniques based on the "weakest link" concept are considered [16–18].

Organosilane and sizing treatments are known to be efficient to protect the fibre surface against moisture attack and as a consequence to enhance fibre properties as well as the hydrothermal resistance of glass fibre reinforced-composites [19]. Surprisingly, although the structure of the deposit and the improvement of the interfacial stress transfer capacity have been of great interest in the litterature, only few studies have been devoted to the effect of the sizing layer on the statistics of glass fibre strengths. By using the double-box distribution, Gomez and Kilgour [20] studied the effect of the chemical structure of alkoxysilane coupling agents on the glass fibres tensile strength. It was reported that an increase in the functionality of the alkoxysilane (i.e. the number of alkoxy groups) results in an increase in the tensile strength and a better protection of the glass surface from the most severe surface flaws. This effect was attributed to a better bonding to the glass surface and by favouring the siloxane network formation. In a previous work [18], we reported the effect of an elastomer-type interphase on the statistic of glass fibre exhibiting single distribution. Fibre strength were found to be well described by a Weibull cumulative distribution function. It appears from the reported papers that statistics studies can be used as an indirect observation technique of the effect of a sizing treatment on fibre flaws.

Properties of fibre-reinforced composites depends not only on the interfacial stress transfer capacity, but also on the mechanical properties of the fibre, which in turn depends on the applied surface treatment. Oxydation treatments in the case of carbon fibres produces different effects [21], i.e. smoothening of the surface, micro-etch pit formation, and introduction of surface functional groups. While the latter provides interfacial stress transfer capacity, the formation of pit can lead to a drastic decrease of fibre tensile strength. As a consequence, a long treatment time, which increases the chemical bonding of the resin to the fibre leads to a decrease in the mechanical properties of the composite material due to fibre surface damage [22]. It appears from the reported studies that when applying a surface treatment in order to improve the interfacial stress transfer capacity, the mechanical properties of the surface-modified fibre are of great importance. In this paper, we attempt to show the effect of organosilane coupling agent and commercial sizing as well as processing on the flaw distribution of multimodal glass fibres.

2. Theoretical background

The three parameter Weibull cumulative distribution function (CDF) is given by the following equation [23]:

$$P(\sigma) = 1 - \exp\left[-\left(\frac{\sigma - \sigma_u}{\sigma_0}\right)^m\right] \qquad (1)$$

where P is the cumulative probability of failure of a fibre at the applied stress σ, m is a shape parameter or the Weibull modulus. σ_0 and σ_u are a scaling parameter and a treshold stress below which the failure probability is zero, respectively. To apply this equation to the failure of glass fibres, several assumptions have to be made [16]:

- fracture is governed by a single flaw population
- the strength is assumed as not time-dependent
- compressive strength does not contribute to fracture

The probability density associated with Equation 1 is given by

$$p(\sigma) = \frac{m}{\sigma_0} \cdot \left(\frac{\sigma - \sigma_u}{\sigma_0}\right)^{m-1} \exp\left[-\left(\frac{\sigma - \sigma_u}{\sigma_0}\right)^m\right] \qquad (2)$$

The parameter σ_u is used to obtain the best correlation with the fitting of the experimental data. However, in practice, the use of the threshold parameter can hide a multimodal distribution and leads to non realistic results [24]. Moreover, values obtained for σ_u are sometimes physically meaningless [5]. Therefore, a two-parameter Weibull statistic is generally used [25–28] by stating $\sigma_u = 0$ as recommended by Trustum and Jakatilaka [29] for brittle materials.

It has been shown [25, 26] that glass fibres exhibit multiple populations of defects with varying gauge length. In this case, single two-parameter Weibull CDF is inappropriate and one must use multimodal distribution. The two-parameter bimodal Weibull CDF, applied by Beetz [28] on carbon fibres is given by:

$$P(\sigma) = 1 - p\,\exp\left[-\left(\frac{\sigma}{\sigma_{01}}\right)^{m_1}\right] + (1-p)\exp\left[-\left(\frac{\sigma}{\sigma_{02}}\right)^{m_2}\right] \qquad (3)$$

where m_1, m_2, σ_1, and σ_2 are the shape and scale parameters of the corresponding population of defects respectively. p is the mixing parameter, i.e. the fraction of failures due to the most severe (type 1) defects. In such a description, it is assumed that no interaction occurs between type 1 and type 2 defects.

Different estimators are generally used to calculate the probability of failure P_i of the ith strength. This problem was discussed in other papers [29–31] as reported by Asloun *et al.* [16] and it can be assumed that the following estimator leads to the less biased m values for number of specimens less than 50:

$$P_i = \frac{i - 0.5}{N} \qquad (4)$$

3. Experimental

3.1. Glass fibres

E-glass fibres have been supplied by VETROTEX Int. Three different types of fibres differing by their surface treatments have been considered:

TABLE I Average value and standard deviation of fibre diameter of the considered E-glass fibres (weight loss was also used to compute the thickness of the sizing layer)

Fibre	Diameter (μm)	Standard deviation (μm)	Weight loss[a] (wt %)	Sizing thickness[b] (nm)
Water-based sizing	18.1	1.4	—	—
A1100 treated	18.3	1.7	0.17	21
P122 1200 Tex	19.1	1.4	0.77	86
P122 2400 Tex	26.6	2.0	0.55	86

[a]Determined from TGA analysis.
[b]Calculated assuming a continuous sizing layer.

- a "water-based sizing" (WS) treatment corresponding to the deposition of an aqueous solution of an antistatic agent.
- a silane based treatment corresponding to the deposition of γ-aminopropyltriethoxysilane (denoted A1100) from an 1 wt % aqueous solution of silane
- Commercial sizing referred P122 by Vetrotex Co., known as a "universal sizing", i.e. suitable for epoxy as well as polyester matrices. The coupling agent included in this sizing formulation was the A1100 (concentration of 1 wt %). Other constituents such as a lubricant and a film former were also included. Two different P122 references, namely 1200 Tex and 2400 Tex, with different fibres diameter have been considered.

The average diameter were measured by optical microscopy with a sample size of 100. Results are given in Table I. The amount of the sizing (by wt.) has been determined by thermogravimetric analysis under inert atmosphere (heating rate: 5 K min^{-1}) and the thickness of the deposit layer was estimated assuming a continuous layer.

3.2. Processing

Details of glass fibres processing are well known and can be found in the literature [32]. As reported by Schmitz and Metcalfe [25], the glass fibre processing can modify the distribution of flaws. According to this work, flaws on a filament extracted from strands are "considerably more severe" than those on a virgin filament.

Strands used were based on several hundred to several thousand filaments assembled after sizing. Additional steps include drying and curing of the sized fiber. In the case of the WS and A1100 fibres, strands were directly wound to form a package. A Roving process has been applied to the P122 one: several strands are mechanically gathered together to form the final strand which is assembled in a bobbin (suitable for filament winding).

3.3. Mechanical testing

Tensile strengths were measured using an Adamel Lhomargy DY22 machine, operating with a cross-speed of 0.5 mm min^{-1}, in a "controlled atmosphere" that is, at a temperature of 22 °C and %RH = 50 since it is known that these parameters can influence the tensile strength of glass fibres [33, 34].

Samples were mounted in a rectangular paper-box and fixed with an epoxy adhesive. Special care has been taken during handling in order to avoid creation of additional defects and changes on flaw distribution. Sample which broke close to the adhesive have not been considered. All tests were conducted at a gauge length of 20 mm.

4. Results

4.1. Sample size

The first requirement that arises with this mode of testing which involves statistical considerations concerns the sample size. In a study dealing with carbon fibres, Asloun *et al*. [16] found that 20 samples are enough to obtain results which are statistically valid. Thus, tests were performed on E-glass fibres by varying the sample size from 10 to 77. The P122 2400 Tex fibres have been selected for that purpose, since this fibre exhibits the greater volume tested for the same gauge length. The sample size required to have representative data will be sufficient for the other type of fibers. The average fibre strength and the standard deviation with respect to sample size are given in Fig. 1.

Values of standard deviation and $\overline{\sigma}_f$ remain nearly constant up to a sample size of 35–40. For the present investigations on the statistics of fibre breaks and the influence of the surface treatments, the variation of standard deviation and $\overline{\sigma}_f$ can be considered as sufficient criteria. As a consequence, the sample size will be considered as equal to about 40.

4.2. Tensile strength

Average tensile strength for a sample size of 40 and a gauge length of 20 mm are given for each type of fibre in Table II. A1100 and WS-treated fibres have quite the same value of tensile strength whereas the tensile strength of P122 1200 Tex fibres is slightly lower although in the standard deviation range. The values obtained for the P122 2400 Tex fibres demonstrate the well known size effect, i.e. a decrease in material strength is

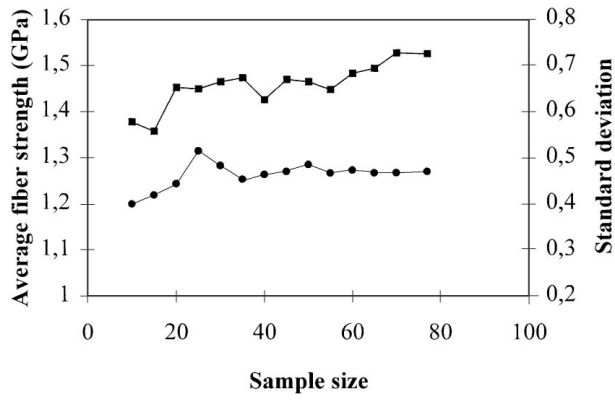

Figure 1 Influence of the sample size, N, on the average tensile strength, $\overline{\sigma}_f$ (■) and the standard deviation (●) of P122 2400 Tex fibres (gauge length of 20 mm).

TABLE II Average tensile strength and standard deviation of different types of E-glass fibres at a gauge length of 20 mm

Fibre	Average tensile strength (GPa)	Standard deviation (GPa)
Water-based sizing	1.92	0.64
A1100 treated	2.02	0.53
P122 1200 Tex	1.75	0.34
P122 2400 Tex	1.42	0.47

TABLE III Values of the shape, scale, and mixing parameter of the bimodal Weibull two parameters cumulative distribution function of different types of E-glass fibres differing from their surface treatments

Fibre	m_1	s_1	m_2	s_2	p
Water-based sizing	99.88	0.77	4.03	9.44	0.10
A1100 treated	163.24	1.37	5.12	7.46	0.09
P122 1200 Tex	175.50	1.49	5.53	5.02	0.12
P122 2400 Tex	97.07	0.68	4.04	6.58	0.09

observed with increasing the size or the volume of the specimens.

4.3. Weibull treatment

4.3.1. General statements

In order to check if the Weibull statistics is appropriate to describe the reported tensile strength values, a modified form of the Equation 1 for $\sigma_u = 0$ is used:

$$\ln\left[\ln\left(\frac{1}{1-P(\sigma)}\right)\right] = m\ln(\sigma) - m\ln(\sigma_0) \quad (5)$$

In that case, $\ln(-\ln(1-P))$ varies linearly with $\ln(\sigma)$ and the Weibull modulus is given by the slope, m. Such a Weibull function supposes that the failure is governed by one type of defects. When considering several categories of defects, rearrangement of Equation 1 can still be used, although it does not result in a straight line as Equation 5. The extreme values should represent two straight lines with different slopes, and the slope change is indicative of multimodal distribution. Such types of dependence are given in Fig. 2 for the different kinds of surface treatments and sizing considered in this study.

The fact that the plots exhibit different slopes implies that failure of the E-glass fibres considered in this study is governed by different types of defects. Deviation from a linear dependence indicates a mixed distribution [25, 26], that is, stress concentrations factors (SCF) distribution of type 1 and type 2 defects are superimposed. In the region of slope change, a mixed distribution based on both type of defects is observed, whereas at the extreme parts of the curve, the distribution is only based on one type of defect. Such effect has been discussed in the studies devoted on S and E-glass fibres by Schmitz and Metcalfe [25, 26]. They used Gaussian and Weibull probability functions and concluded that the fibres exhibit multiple modes of failure with varying gauge length. More recent studies [5, 17, 18, 35] showed that Weibull CDF can also be appropriated for describing the failure of E-glass fibres.

In our case, failure at a gauge length of 20 mm is governed by two type of defects, as indicated by the two-slope curves given in Fig. 2 and a Weibull bimodal CDF can be used.

4.3.2. Mathematical treatment

Parameters of the Weibull bimodal distribution are determined by a classical least-squares method. Results are given in Table III and the ability of the Weibull function to fit the experimental data can be evaluated graphically in Fig. 3 (Weibull probability paper). It can be noticed that the cumulative bimodal Weibull two parameters distribution function is suitable for the description of the failure of the E-glass fibres considered in this study at 20 mm gauge length.

5. Discussion

5.1. General statements

As reported by Schmitz and Metcalfe [25, 26], the failure of glass fibres is governed by several types of flaws with varying gauge length. Failure modes have been attributed to three populations of defects in the range 0.5–500 mm. The third category appears at a gauge length smaller than 1 mm. Rosen [36] performed tensile strength measurements at three different gauge lengths and proposed the "double box distribution", i.e. the glass fibre can be described in terms of a fraction with minor flaws and a fraction with severe flaws. Gauge lengths vary from 5 to 130 mm. The results reported in this study showing two populations of flaws for a 20 mm gauge length are in agreement with those studies.

Nevertheless, glass fibres have not been studied so much since these early works and the other studies reported in the literature are devoted to the environment during testing [33], the theoretical consideration on the statistic of failure [35, 37] or the evaluation of the statistical parameters of a Weibull distribution [38]. In a previous study [18], the effect of an elastomer-based interphase on glass fibre strength was reported. Fraction of severe defects were too weak to be taken into account and mathematically treated. As reported by Beetz [28], as the mixing parameter is greater than 0.9 or smaller than 0.1, one of the modes is clearly dominant and a unimodal approximation is reasonable. Even if a unimodal distribution is considered, the effect of surface treatment can be appreciated. By taking both modes into account (even if p is about 0.1), the effect of the surface treatment of the glass fibres, i.e. the physicochemical interactions between the sizing components and glass surface as well as the possible effect of processing of fibres can be evaluated.

5.2. On the scale and shape parameters

Before discussing the origin of the two populations of defects, the significance of the variation of the shape parameter or Weibull modulus, m, and the scale parameter, σ_0 need to be precised. According to Schmitz

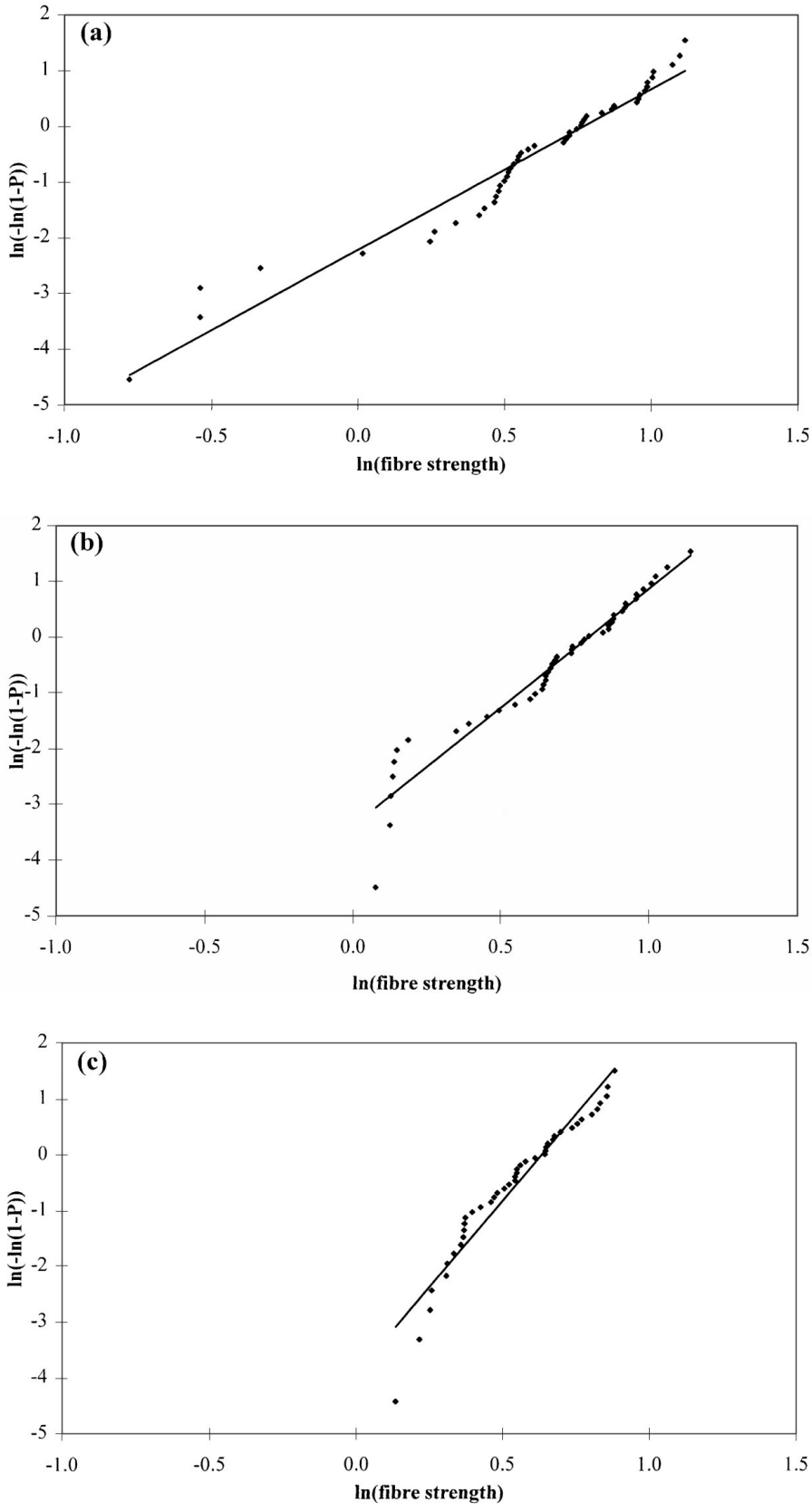

Figure 2 Weibull plot of differents types of E-glass fibre strengths (gauge length of 20 mm): (a) water-sized fibres; (b) A1100 treated; (c) P122 1200 Tex; (d) P122 2400 Tex.

and Metcalfe, two parameters are required in order to describe a population of defects, namely "severity of defect and separation", which are, considering a Gaussian distribution, the mean of the distribution and the standard deviation respectively. Weibull formalism is different, and the authors already stated that m cannot be a parameter for fibre strength. Shape and scale parameters possess a kinetic interpretation and more details are given in reference [39]. In this study, our attempt is only to give some trends for the interpretation of the variations of m and σ_0 reported in Table III.

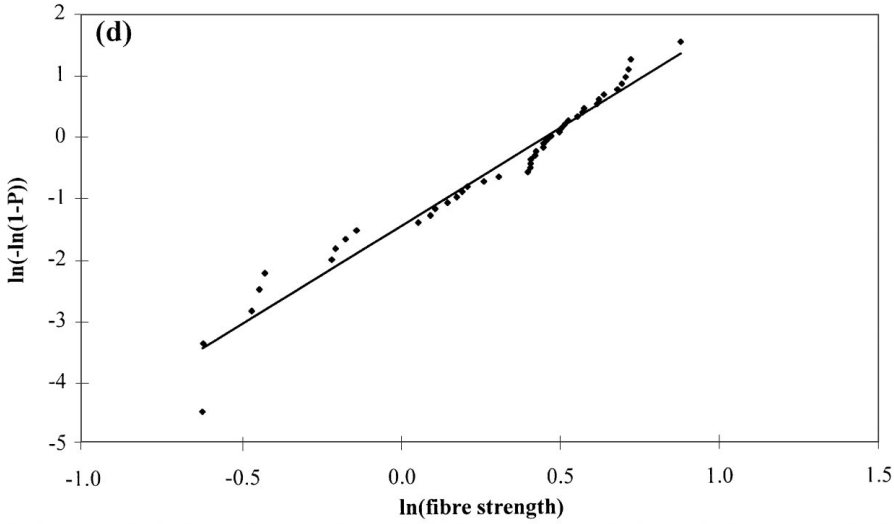

Figure 2 (*Continued*).

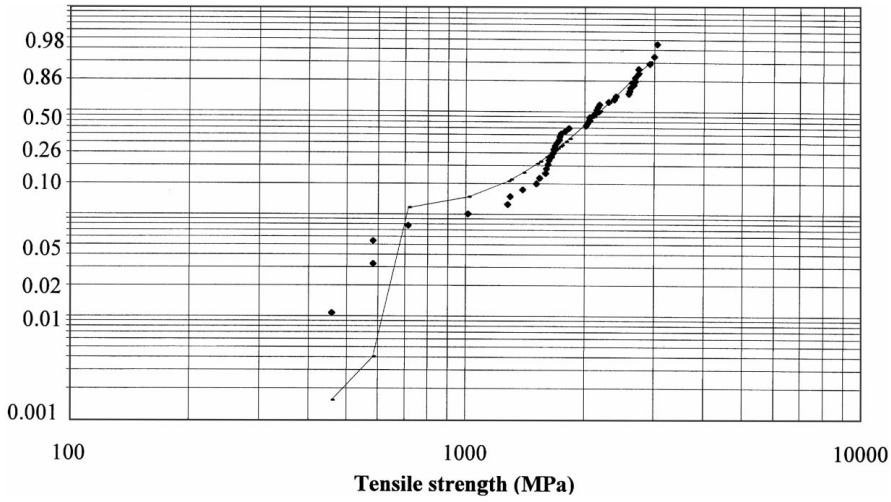

(a)

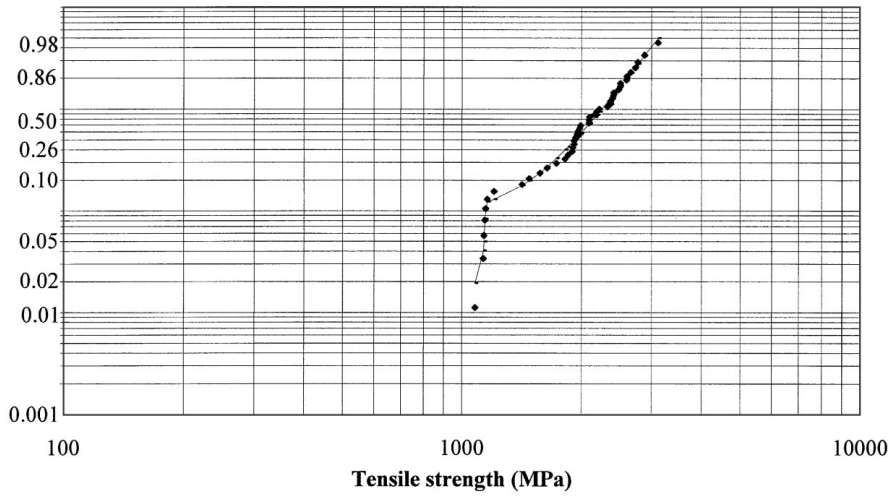

(b)

Figure 3 Fitting of the experimental data with a bimodal Weibull two parameters cumulative distribution function: (a) water-sized fibres; (b) A1100 treated; (c) P122 1200 Tex; (d) P122 2400 Tex. (*Continued*)

Figs 4 and 5 display the theoretical probability density (Equation 2) in the case of a unimodal distribution with varying shape and scale parameters. The influence of m is quite similar in both cases: $\sigma = 1$ and $\sigma_0 = 7$. Severity decreases with increasing m at low values and then remains at the σ_0 value. As a consequence the scale parameter should be representative of the mean stress concentration factor for m values greater than 4–5. In

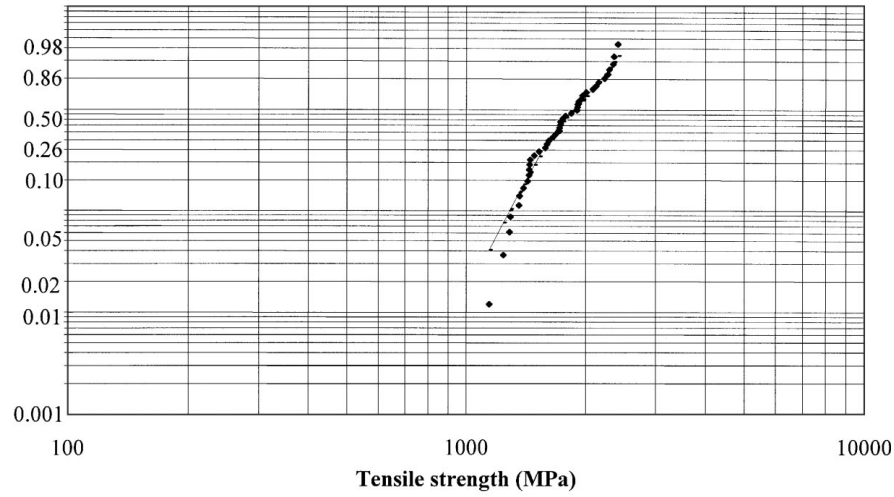

(c)

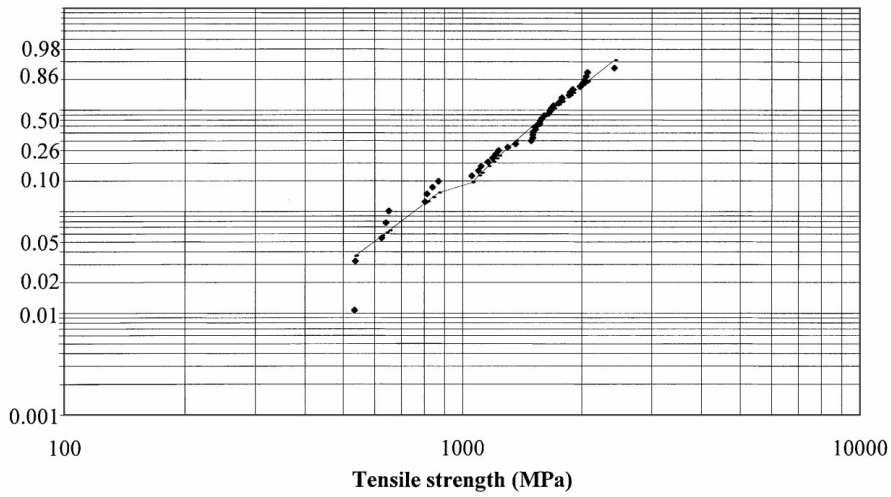

(d)

Figure 3 (*Continued*).

this range, the changes of m are more representative of the separation than the severity. $m < 3.44$ gives a positively skewed distribution ($m > 3.44$ gives a negatively skewed one). For $m = 3.44$, the distribution is normal. An increase of the value of the scale parameter is representative of a slight increase of the separation when m remains constant.

m and σ_0 are both related to separation and severity. However, if one of the parameters remain constant, or if the changes are important, a qualitative interpretation is possible. As a consequence, according to the range of our experimental results, the Weibull modulus is more representative of the separation thus of the homogeneity of the flaws, whereas the scale parameter is related to the severity of the distribution.

5.3. Identification of the distributions

Fig. 6 displays the Weibull plot of the different type of fibres. A1100 and WS treated fibres have been fabricated without using the Roving process. The behaviour for stresses greater than 2 GPa is quite similar. For the A1100-treated fibres, type 1 is dominant up to 1.2 GPa and a mixed distribution is observed between the two values. The main difference between the two types of glass fibres is the type 1 distribution which is shifted to higher tensile stresses, and the slope which is more pronounced as revealed by the value of m_1. If we assume that the coating layer does not influence the volume flaw distribution (or in a weaker way than the surface flaws), the type 1 defects are localised on the surface, whereas the second population are some types of internal defects or surface defects which are not influenced by the coating. This will be developed hereafter. The difference between WS and the A1100-treated fibres in the 0.5 GPa range is the transition zone between type 1 and type 2 defects.

5.4. Effect of the deposition

We assume that, after the spinning process from the molten state and before the sizing deposition, the flaw distribution can be assumed to be similar for fibres of the same diameter. Separation of type 1 defect for A1100-treated fibres is narrower than that of the WS fibres and flaws are less severe as revealed by the values

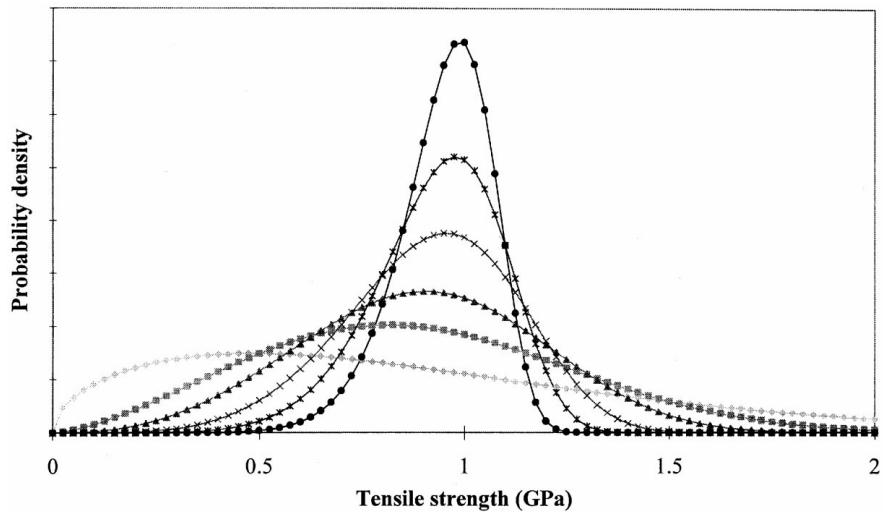

(a)

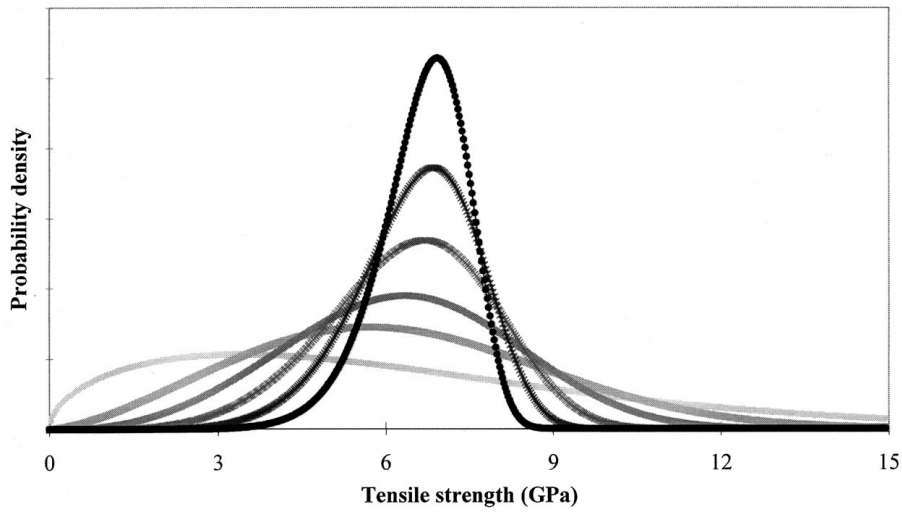

(b)

Figure 4 Effect of the changes of the shape parameter, m, on the unimodal Weibull two-parameter probability density for values of the scale parameter σ_0 equal to 1 (a) and 7 (b). (–♦–): $m = 1.5$; (–■–): $m = 2.5$; (–▲–): $m = 3.44$; (–×–): $m = 5$; (–∗–): $m = 7$; (–●–): $m = 10$.

of the shape and scale parameters. This effect can be associated with the following mechanisms:

1. If we assume that new flaws can not be created even while handling, then the sizing layer should prevent deterioration of pre-existing defects due to handling and/or fibres/fibres contacts in contrast with WS fibres which are more sensitive to moisture. This degradation should affect severity as well as separation.

2. Considering a fracture mechanics approach, and assuming a SCF distribution, the presence of sizing increases the mean "apparent" SCF and favours the more homogeneous flaws. Indeed, before reaching the value of critical stress intensity factor (CSIF), one as first to deform or to break the crosslink, i.e. a siloxane bond. Then only break issued from surface flaws occurs. The fact that the low stress part of the type 1 distribution is more shifted than the highest one provides another argument. The network deformation (or fracture) will play an important role for low stress defect, by giving an "apparent" SCF which is greater than the real one. Whereas at high stress level, when reaching the value of the CSIF, the network should already be deformed or broken. As a consequence, apparent and real SCF should be equal. This phenomenon should also affect sub-critical crack growth.

This can be also viewed as a disappearance of the severe surface flaws by the three-dimensional graded network issued from the interaction between the organosilane and the glass fibre surface. This healing can be understood as an increase of the crack tip radius, the flaw after surface treatment being either elliptical than sharp. Severe surface flaws could be "filled" by the aminosilane, as shown in Fig. 7. The resulting SCF distribution (in both cases A1100 and P122 1200 Tex) is very sharp and it appears some kind of threshold phenomenon. It is more likely to attribute this threshold to defects which are not affected by the surface treatment rather than to healed defects which should show a larger SCF distribution. This is analytically discussed in Appendix A.

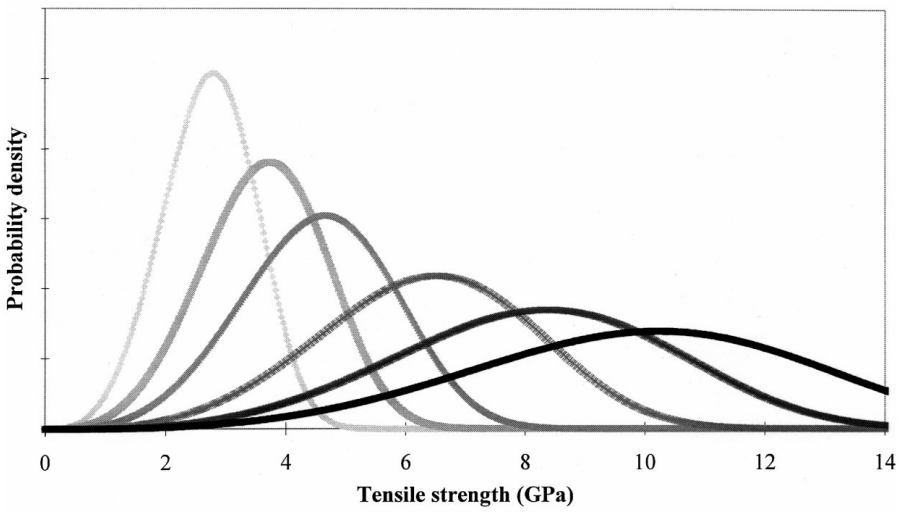

(a)

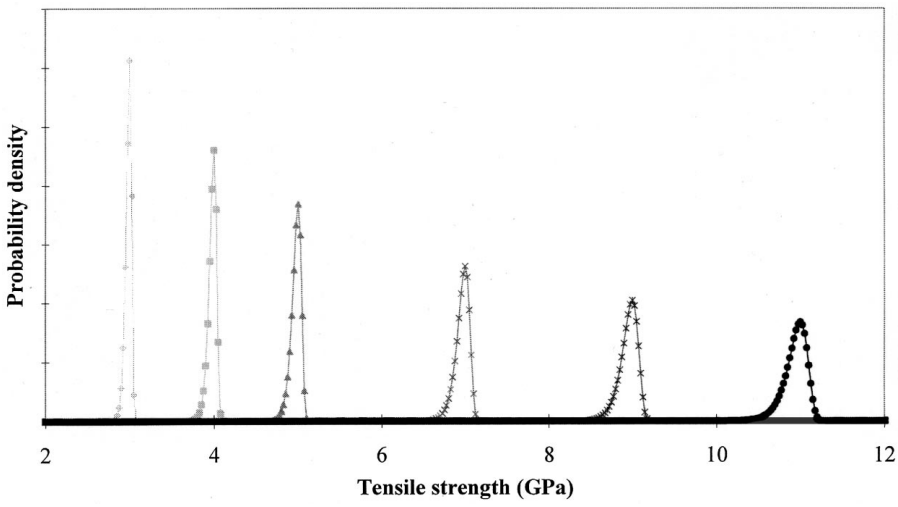

(b)

Figure 5 Effect of the changes of the scale parameter, σ_0, on the unimodal Weibull two-parameter probability density for values of the shape parameter m equal to 4 (a) and 100 (b). (–♦–): $s = 3$; (–■–): $s = 4$; (–▲–): $s = 5$; (–×–): $s = 7$; (–∗–): $s = 9$; (–●–): $s = 11$.

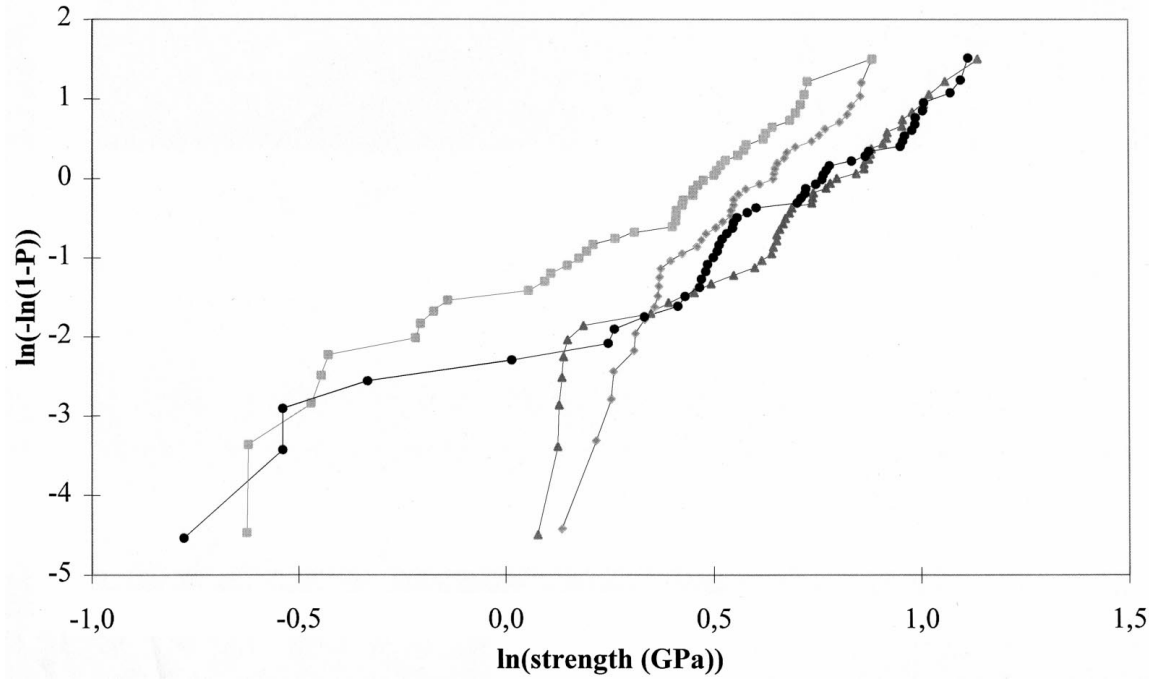

Figure 6 Weibull plots for E-glass fibres with differents surface treatments in a comparative way.

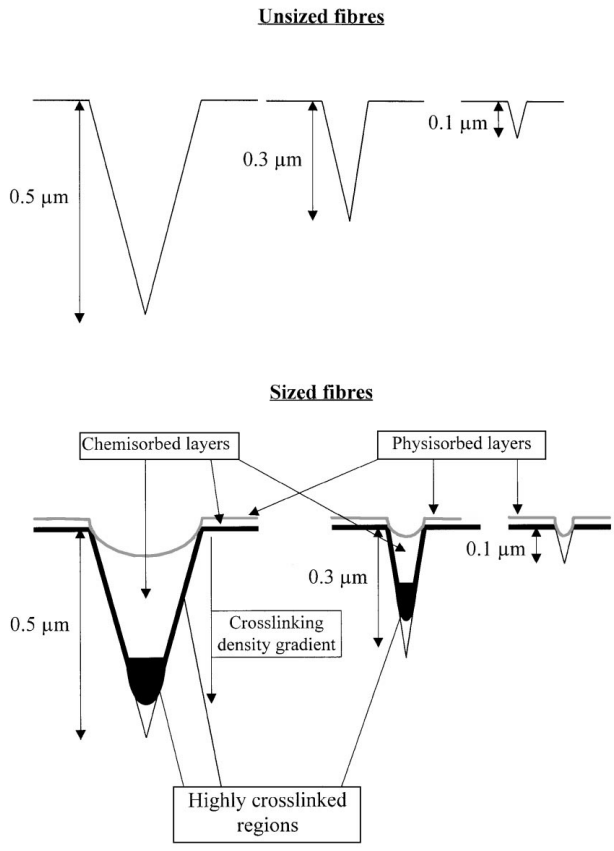

Figure 7 Schematical representation of flaws; effect of a surface treatment.

By using the relationship between the toughness of the material (taken as 0.7 MN $m^{-3/2}$ for soda lime glass), the fracture stress and the crack dimension for a single-edge notch specimen (see Appendix A), the size of the surface defect on a WS fibre ranges approximately from 0.5 to 0.05 μm. A value of 0.1 μm is obtained for the threshold after a surface treatment. Thus, flaws of dimensions less than 100 nm are not healed by the surface treatment and lead to the observed threshold phenomenon.

This is to relate with the structure of aminosilane coupling agents in the deposit solution, generally an aqueous solution. Ishida *et al*. [40] measured the hydrodynamic radii of hydrolysed γ-APS at various concentrations by quasielastic laser light scattering spectroscopy. Measured dimensions were in the 150 nm order for a solution of 1% γ-APS by weight and were attributed to aggregates of small molecules rather than unseparable molecular species. Thus, healing should be efficient for flaws whose dimensions enable sufficient interactions with the coupling agent aggregates in the aqueous solution. Thus we can introduce the concept of a *critical dimension* up to which defects are not healed, i.e. interactions between the flaw and the aggregates are not sufficient. The value of this critical dimension derived from LEFM considerations (in the 100 nm range) is in good agreement with the measured dimensions of the γ-APS molecular species in a 1wt% aqueous solution (150 nm) [40].

Unexpected behaviour is observed for the P122 1200 Tex fibres at high stresses. Indeed, volume flaws seem to be more severe than those from A1100 and WS fibres. This effect can be due to the Roving process, since the sizing does not largely affect type 2 defects as revealed by the comparison between A1100 treated and WS-sized glass fibres. That means that industrial process affects the flaw distribution and that the sized fibres, which are more protected against handling and environmental moisture are also weaker after processing.

The value of the mixing parameter remains quite constant. That means that the amount of type 1 surface defects is not affected by neither the sizing process nor the roving one. Thus, new surface defects are not created during processing, only the pre-existing ones are modified.

It is there demonstrated that the use of statistics is a powerful tool for the understanding of the fibre failure mechanisms and the reinforcement by a surface treatment. The combination of this approach with the more deterministic LEFM one enable to "observe" inherent flaws which often can not be systematically detected by non destructive methods. Both approaches should thus be considered as *complementary*: the probabilistic scheme is able to describe the size effect, but avoid any physical consideration about the flaws. This is possible via the LEFM theory, which in turn does not explain the decrease in strength associated with an increase of specimen size.

An analogy can be done between the effect of sizing treatment and the glass strengthening of silica glass by thin gel-derived coatings [41]. In fact, the radius of the cracks on silicate glass surfaces generated during glass processing can be increased by the attack of acidic solutions [42] or by healing using a sol-gel

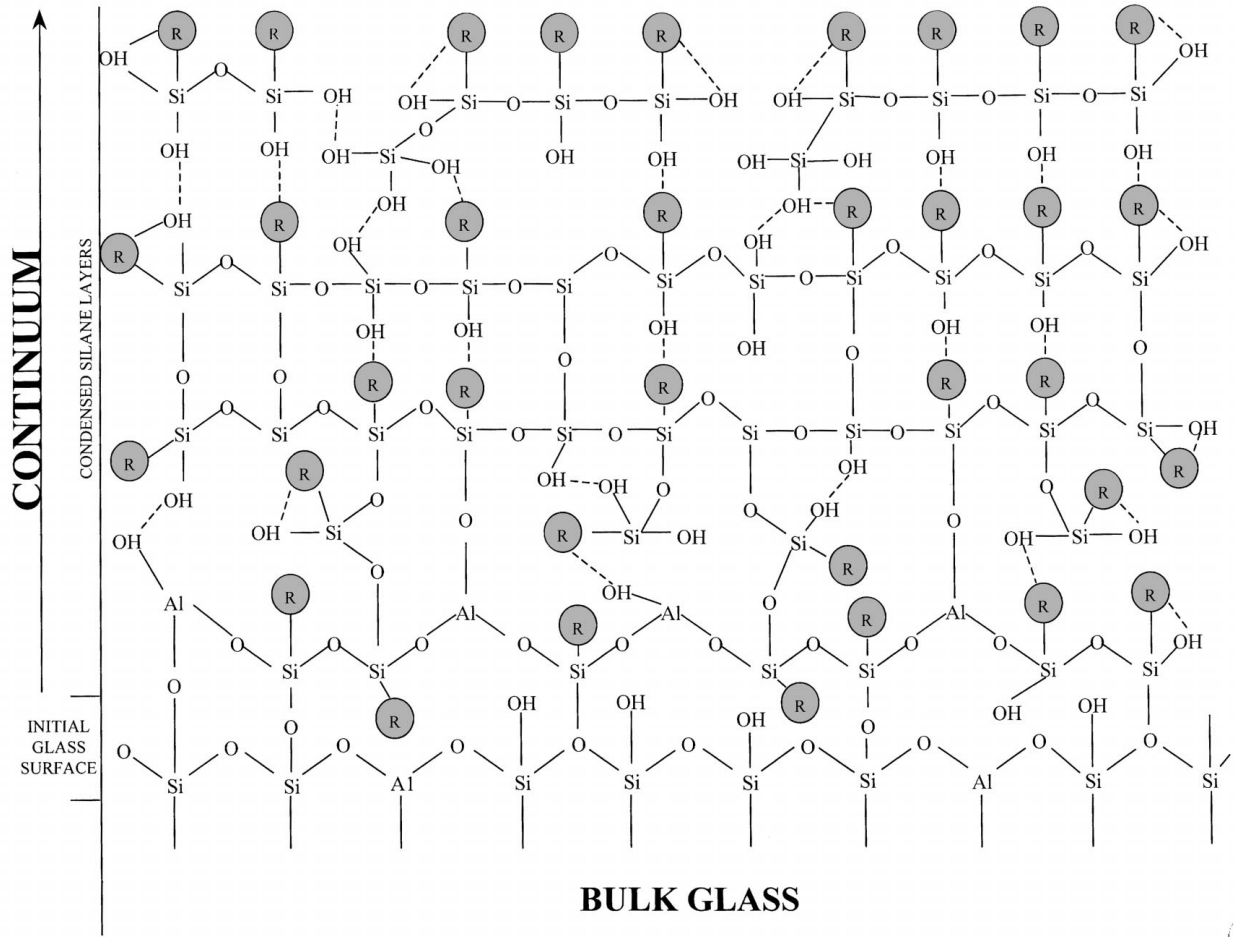

Figure 8 Schematic diagram of γ-aminopropyltriethoxysilane layer on an E-glass fibre: (---) hydrogen bonds; R is NH_2 (CH_2).

deposit [41, 43–45]. It was demonstrated that such layers synthesised from alkoxysilanes can fill the cracks leading increase the radius of the curvature at the defect tip. Such phenomenon can be evoked for the healing of glass fibres surface flaws by the sizing layer. In addition, according to the chemical components from the sizing formulation, i.e. the film former—a polymer—and the coupling agent—the γ-aminopropyltriethoxysilane—, the resulting layer is very similar to those obtained from the sol-gel chemistry of hybrids [46]. In fact, it is well known that a continuum exists from the glass surfaces—reacted silanols—to the polysiloxane network resulting from the condensation of hydrolyzed ethoxy species of the silane [2] as shown in Fig. 8. Thus, such a kind of molecular architecture is close to that of hybrid organic–inorganic coatings on glass.

6. Conclusion

This work on the characterisation of coatings on E-glass fibres has shown that:

- Failure of E-glass fibre at a gauge length of 20 mm is governed by two types of defects and Weibull bimodal cumulative distribution function is suitable for the description of experimental data.
- The most severe flaw population is localised at the glass fibre surface, whereas type 2 defect are supposed to be internal ones.
- Coupling agent and sizing treatments recover surface defects, by diminishing separation as well as severity. This effect can be associated to the creation of polysiloxane network on the glass surface, and has been interpreted in terms of flaw healing via a combination of probabilistic and deterministic theories. An analogy has been proposed between the sizing treatment of glass fibres and the strengthening of silica glass by means of hybrid organic-inorganic coatings.
- Sizing influence neither internal flaws directly, nor amount of surface defects.
- Industrial process can affect internal flaw distribution.

Acknowledgements

DER/EDF is acknowledged for its financial support and Vetrotex International for supplying E-glass fibres. The authors want to thank Profs D. Rouby and H. Sautereau for very helpful discussions.

A. Appendix A: Linear elastic fracture mechanics and glass fibres flaws

A.1. Representation of the flaws

To obtain information about dimensions of the flaws, we have assumed the general shape of a surface defect according to the presence of a surface treatment or not:

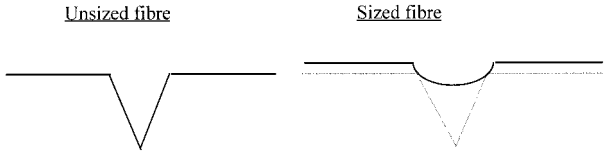

In other words, to explain the presence of the threshold value, it is assumed that the effect of the sizing is to increase the crack tip radius. Based on this assumption, WS fibres were treated in the LEFM frame as a single-edge notch specimen (SEN) and A1100/P122 as elliptical cracks (scale is not respected).

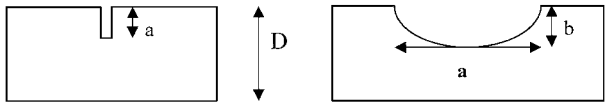

A.2. Analytical treatment

The following is taken from the works of Williams [47].

A.2.1. Unsized fibres

For an infinite plate containing a crack of length $2a$,

$$K_I = \sigma\sqrt{\pi a} \tag{A1}$$

For our purpose which deals with finite dimensions, a length factor appears. If we define a width factor as D, the diameter of the fibre, we have

$$K_I^2 = Y^2\left(\frac{a}{D}\right)\sigma^2 a \tag{A2}$$

An approximation of Y^2 for SEN and DEN (double edge notch specimen) issued from the analytical result obtained for a periodic array of collinear cracks is given by [48]:

$$Y^2 = 3.94\left(\frac{2D}{\pi a}\right)\tan\left(\frac{\pi a}{2D}\right) \tag{A3}$$

Combination of Equation A2 with Equation A3 gives for the critical flaw size of an unsized fibre:

$$a = \frac{2D}{\pi}\arctan\left(\frac{K_I^2\pi}{3.94\sigma^2 2D}\right) \tag{A4}$$

It should be noticed there that bending effects due to the lack of symmetry (SEN specimen) are not taken into account.

A.2.2. Sized fibres

For an elliptical surface flaw under uniform tension, we have:

$$K_I = \frac{1}{E_2}\sigma\sqrt{\pi b} \tag{A5}$$

where E_2 is a complete elliptic integral of the 2nd kind. Values of E_2 are tabulated in [41] for various radii of b/a. There is no bending effect as for SEN specimen and finite width effects can be approximated by scaling the factor π/E_2^2 by the double edge notch Y^2 given in Equation A3. Thus we have for the critical flaw size of an sized fibre:

$$b = \frac{2D}{\pi}\arctan\left(\frac{K_I^2\pi\cdot E_2^2}{3.94\sigma^2 2D}\right) \tag{A6}$$

b is determined for various values of E_2 which in turn gives the value of a.

A.2.3. Numerical treatment

For unsized fibre, failure stress of distribution I varies from 0.5 GPa to approximately 1.2 to 1.4 GPa. Up to this range, the distributions are mixed. This leads to flaws size varying from 63 nm to 497 nm, thus in the range 0.05–0.5 μm.

For A1100 fibres, the threshold is in the 1.15 GPa order. If we attribute this value to defects which are not affected by the surface treatment, the size obtained according to Equation A4 is 94 nm. If the threshold is attributed to healed defects of distribution I, then we have different combination according to the b/a radius.

a (nm)	971	519	377	311	276	256	243	236	233	232
b (nm)	97	104	113	125	138	153	170	189	210	232

Using the argument of the sharpness of the SCF distribution in the threshold range which is not in agreement with the SCF distribution which would result from the healing of the type I defects owing to their size variability (distribution I of WS), as well as the hypothetical values of a and b obtained in the table, the more realistic physical interpretation of the threshold is that those defects are not affected by the surface treatment.

References

1. F. R. JONES, *Key Eng. Mater.* **116–117** (1996) 41.
2. D. WANG and F. R. JONES, *Surf. Interface Anal.* **20** (1993) 457.
3. Y. ECKSTEIN, *J. Adhes. Sci. Technol.* **2** (1988) 339.
4. E. P. PLUEDEMANN, "Silane Coupling Agents" (Plenum Press, New York and London, 1982).
5. C. AHLSTROM, PhD thesis, Institut National des Sciences Appliquées, France, 1988.
6. W. A. FRASER, F. H. ANCKER, A. T. DIBENEDETTO and B. ERLIBIRLI, *Polym. Compos.* **4** (1983) 238.
7. A. N. NETRAVALI, P SCHWARTZ and S. L. PHOENIX, *ibid.* **10** (1989) 385.
8. M. R. PIGGOTT, P. S. CHUA and D. ANDISON, *ibid.* **6** (1985) 242.
9. M. R. PIGGOTT, *ibid.* **8** (1987) 291.
10. L. GONON, A. MOMTAZ, D. VAN HOYWEGHEN, B. CHABERT, J. F. GERARD and R. GAERTNER, *ibid.* **17** (1996) 265.
11. H. HO and L. T. DRZAL, *Composites* **27A** (1996) 961.
12. V. LACRAMPE, PhD thesis, Institut National des Sciences Appliquées, France, 1992.

13. M. P. NEMETH, C. T. HERAKOVICH and D. POST, *Compo. Technol. Rev.* **5** (1983) 61.
14. P. ZINCK, V. LACRAMPE and J. F. GERARD, *Revue des Composites & Materiaux Avances* **7** (1997) 31.
15. J. F. GERARD, *Polym. Eng. Sci*. **28** (1988) 568.
16. EL M. ASLOUN, J. B. DONNET, G. GUILPAIN, M. NARDIN and J. SCHULTZ, *J. Mater. Sci*. **24** (1989) 3504.
17. B. YAVIN, H. E. GALLIS, J. SCHERF, A. EITAN and H. D. WAGNER, *Polym. Compos.* **12** (1991) 436.
18. C. AHLSTROM and J. F. GERARD, *ibid*. **16** (1995) 305.
19. J. L. KOENIG and H EMADIPOUR, *ibid.* **6** (1985) 142.
20. J. A. GOMEZ and J. A. KILGOUR, Technical Note, Osi Specialties, Inc., 1993.
21. L. M. MANOCHA, *J. Polym. Sci*. **17** (1982) 3039.
22. O. P. BAHL, R. B. MATHUR and T. L. DHAMI, *Polym. Eng. Sci*. **24** (1984) 455.
23. W. WEIBULL, *J. Appl. Mech*. **18** (1951) 293.
24. EL M. ASLOUN, PhD thesis, Université de Haute Alsace, France, 1991.
25. A. G. METCALFE and G. K. SCHMITZ, in Proceedings of the A.S.T.M, (1964) Vol. 64, p. 1075.
26. G. K. SCHMITZ and A. G. METCALFE, *Mater. Res. Stand* **7** (1967) 146.
27. J. W. HITCHON and D. C. PHILLIPS, *Fibre Sci. Tech* **12** (1979) 217.
28. C. P. BEETZ, *ibid.* **16** (1982) 45.
29. K. TRUSTUM and A. S. JAKATILAKA, *J. Mater. Sci.* **14** (1979) 1080.
30. B. BERGMAN, *J. Mater. Sci. Lett*. **3** (1984) 689.
31. *Idem., ibid.* **5** (1986) 611.
32. VETROTEX, *Les Cahiers du Plastique Armé* **7714** (1978).
33. J. A. BURGMAN and E. M. HUNIA, *Glass Technol.* **11** (1970) 147.
34. S. SAKAGUCHI, T. KIMARU and S. TAKAHASHI, Advances in Ceramics, Vol. 2, Physics of Fiber Optic, edited by B. BENDOW (Colombus, Ohio, 1981) p. 140.
35. P. K. GUPTA, *J. Amer. Ceram. Soc* **70** (1987) 486.
36. B. W. ROSEN, "Fiber Composite Material" (ASM, Metals Park, Ohio, 1965) chap: 3.
37. K. K. PHANI, *J. Mater. Sci* **23** (1988) 1189.
38. M. R. GURVICH, A. T. DIBENEDETTO and A. PEGORETTI, *ibid.* **32** (1997) 3711.
39. H. D. WAGNER, *J. Polym. Sci., Polym. Phys*. **27**(1) (1989) 115.
40. H. ISHIDA, S. NAVIROJ, and S. K. TRIPATHY *et al., ibid.* **20** (1982) 701.
41. B. D. FABES, W. F. DOYLE, B. J. J. ZELINSKI, L. A. SILVERMAN and D. R. UHLMAN, *J. Non-Cryst. Solids* **82** (1986) 349.
42. T. P. DABBS and B. LAWN, *J. Amer. Ceramic. Soc.* **65**(3) (1982) C37.
43. J. L. BESSEDE, PhD thesis, Institut National des Sciences Appliquées, France, 1990.
44. H. KADDAMI, S. CUNEY, J. P. PASCAULT and J. F. GERARD, in "Organic Coatings," edited by P. C. LACAZE (Amer. Inst. Phys. AIP 354, 1995) p. 522.
45. F. SURVIVET, "Matériaux Hybrides" (OFTA Arago 17, Masson, Paris, 1996).
46. C. J. BRINKER and G. SCHERER, "Sol-Gel Science, The Physics and Chemistry of Sol-Gel processing" (Academic Press, San Diego, 1989).
47. J. G. WILLIAMS, "Fracture Mechanics of Polymers" (Ellis Horwood Limited, 1984).
48. W. T. KOITER, *Ingenieur Archiv*. **28** (1959) 168.

Received 5 August
and accepted 21 October 1998